Journal of
MATERIALS RESEARCH

Mechanical properties of $Zr_{57}Nb_5Al_{10}Cu_{15.4}Ni_{12.6}$ metallic glass matrix particulate composites

R.D. Conner, H. Choi-Yim, and W.L. Johnson
W.M. Keck Laboratory of Engineering Materials, California Institute of Technology, Pasadena, California 91125

(Received 7 May 1998; accepted 3 May 1999)

To increase the toughness of a metallic glass with the nominal composition $Zr_{57}Nb_5Al_{10}Cu_{15.4}Ni_{12.6}$, it was used as the matrix in particulate composites reinforced with W, WC, Ta, and SiC. The composites were tested in compression and tension experiments. Compressive strain to failure increased by more than 300% compared with the unreinforced $Zr_{57}Nb_5Al_{10}Cu_{15.4}Ni_{12.6}$, and energy to break of the tensile samples increased by more than 50%. The increase in toughness came from the particles restricting shear band propagation, promoting the generation of multiple shear bands and additional fracture surface area. There was direct evidence of viscous flow of the metallic glass matrix within the confines of the shear bands.

I. INTRODUCTION

Amorphous alloys were first discovered by Duwez at Caltech in 1960.[1] This metallic glass requires a high cooling rate (~10^6 K s^{-1}) and can only be produced as thin films. Continued research led to the development of metallic glasses with low (1–10^3 K s^{-1}) critical cooling rates that can be cast as ingots with large (centimeter) minimum dimensions.[2] One of the bulk amorphous alloys developed at Caltech has the nominal composition $Zr_{57}Nb_5Al_{10}Cu_{15.4}Ni_{12.6}$.

$Zr_{57}Nb_5Al_{10}Cu_{15.4}Ni_{12.6}$ has mechanical properties similar to other bulk metallic glasses,[3,4] such as high strength (~1.8 GPa), high elastic limit (~2%), moderate stiffness (85 GPa), and a tendency to fail catastrophically along narrow shear bands. In an effort to increase the toughness of this metallic glass while retaining desirable mechanical properties, $Zr_{57}Nb_5Al_{10}Cu_{15.4}Ni_{12.6}$ was combined with particulate reinforcements to make metallic glass matrix/particulate composites. Ductile metals have been shown to improve the toughness in traditional oxide glasses,[5–8] and Zr–Al–Ni–Cu metallic glass reinforced with ZrC showed increases in Young's modulus, compressive strength, compressive plastic elongation, and hardness.[9] The particles interact with the propagating shear band, causing it to slow (or stop) and deflect, thus delaying failure and improving toughness. The properties of $Zr_{57}Nb_5Al_{10}Cu_{15.4}Ni_{12.6}$ and the various ceramic particles and refractory metals used as reinforcement are listed in Table I.

This article reports on the measured mechanical properties of $Zr_{57}Nb_5Al_{10}Cu_{15.4}Ni_{12.6}$ metallic glass and $Zr_{57}Nb_5Al_{10}Cu_{15.4}Ni_{12.6}$ matrix particulate composites. The particulate reinforcement increased the toughness of $Zr_{57}Nb_5Al_{10}Cu_{15.4}Ni_{12.6}$ in both tension and compression experiments. Multiple shear banding in composite compression specimens allows a 300% increase in strain to failure compared with monolithic $Zr_{57}Nb_5Al_{10}Cu_{15.4}Ni_{12.6}$ samples. A 50% increase in the tensile energy to break of $Zr_{57}Nb_5Al_{10}Cu_{15.4}Ni_{12.6}$ is measured for composite tensile samples. Direct evidence exists that the metallic glass undergoes viscous flow within the propagating shear band.

II. EXPERIMENTAL

Ingots of $Zr_{57}Nb_5Al_{10}Cu_{15.4}Ni_{12.6}$ metallic glass were prepared by arc-melting elemental metals in a Ti-gettered argon atmosphere. Metal purity ranged from 99.7% for zirconium to 99.999% for copper (metals basis). The metallic glass ingots were combined with the second

TABLE I. Properties of $Zr_{57}Nb_5Al_{10}Cu_{15.4}Ni_{12.6}$ and selected reinforcing particles.

	Young's modulus (GPa)	Shear modulus (GPa)	Poisson's ratio (ν)	Thermal expansion (α) (10^{-6}/°C)	Nominal strength (MPa)
$Zr_{57}Nb_5Al_{10}Cu_{15.4}Ni_{12.6}$	84.7	30.8	0.376	8.7	1800[a] 1200[b]
Tungsten	411	160	0.280	4.6	σ_y ~ 725 σ_u ~ 1000
Tantalum	186	69	0.342	6.5	σ_y ~ 350
Silicon Carbide	411	174	0.185[c]	6.5	35–138 @ 25 °C

[a]Uniaxial compression.
[b]Uniaxial tension.
[c]Self-bonded.

phase particles by induction melting and mixing on a water-cooled copper crucible in a Ti-gettered argon atmosphere. The composite ingots were then vacuum-induction melted in a quartz crucible and injected into a copper mold by use of argon at 207 kPa. Table II lists the particle type, size, and volume fraction (V_f) for each of the composites tested. Full details of the processing are given elsewhere.[10]

Compression test samples were fabricated by casting the composite ingots into 3-mm diameter rods. The rods were cut to 6-mm lengths with an Isomet saw equipped with a diamond blade. The cut rods were mounted in a collect holder that was clamped in a V block, and the ends were lapped flat and square to the axis on SiC wet-dry sand paper, with a final polish using 600 grit. The flatness and perpendicularity of the faces was checked by clamping the polished rod in a micrometer and examining the gap at 40× magnification with a binocular microscope. Tensile test specimens were cast in a dogbone-shaped mold. The 21-mm gauge length of the dogbone ingot was then ground into a rectangle 2.4 mm wide and 1 mm thick.

Quasi-static compression and tension tests were performed on an Instron 4204 load frame at a crosshead speed of 0.5 mm/min. A compression test fixture was used to ensure axial loading. The test specimens were compressed between tungsten carbide platens, with the faces lubricated to reduce friction at the ends and prevent sample barreling. The flared ends of the tensile test specimens fit into matching recesses in the tensile grips, which were attached to the Instron machine by universal joints. Strain was measured with a calibrated extensometer.

The fracture surfaces of the tested samples were examined with scanning electron microscopy (SEM). Light microscopy was used to evaluate particulate distribution.

A Perkin-Elmer Series 7 thermomechanical analyzer was used to measure the thermal expansion coefficient of $Zr_{57}Nb_5Al_{10}Cu_{15.4}Ni_{12.6}$. Elastic constants of the $Zr_{57}Nb_5Al_{10}Cu_{15.4}Ni_{12.6}$ metallic glass were measured with a Parametrics Model 5052UA ultrasonic analyzer connected to an oscilloscope for data analysis. The measured physical properties of the matrix and reinforcement materials allowed the calculation of composite elastic modulus and residual stress with the Eshelby equivalent inclusion method.[11,12] Density measurement was by the hdyrostatic weighing technique.[13] X-ray diffraction patterns of the materials were obtained using an Inel diffractometer with a position sensitive detector and Co K_α radiation (wavelength = 0.1790 nm).

TABLE II. Particle reinforcement type, size, and volume fraction used in the $Zr_{57}Nb_5Al_{10}Cu_{15.4}Ni_{12.6}$ metallic glass matrix/particulate composites tested.

Particle	W	W	WC	Ta	SiC	SiC
Size (μm)	150	3, 12	50	40	37	80
V_f (%)	5, 10, 15	5, 10	5, 10	10	10	10, 20

III. RESULTS

Microscopy reveals uniform reinforcement distribution is typical of all the composites tested. Sample porosity is minimal, despite a few small pits adjacent to the particles. No crystals are visible in the metallic glass matrix, and the matrix/particle interface is smooth, indicating a shallow interface layer. X-ray analysis showed that all the composites tested retained an amorphous matrix.

The elastic modulus of unreinforced $Zr_{57}Nb_5Al_{10}Cu_{15.4}Ni_{12.6}$, measured using the slope of the stress–strain curve, Fig. 1, is 83 GPa in tension and 85 GPa in compression. This is in good agreement with E = 84.7 GPa measured with the ultrasonic technique. The elastic moduli of the composite samples were taken from the slope of the stress-strain curves. Figure 2 is a graph of the measured elastic moduli versus the calculated values.

Compression tests were conducted on monolithic $Zr_{57}Nb_5Al_{10}Cu_{15.4}Ni_{12.6}$ and particulate composites containing tungsten, tungsten carbide, tantalum, and silicon carbide. All the compression samples fail along shear bands oriented at 45 degrees to the axial loading direction.

Unreinforced $Zr_{57}Nb_5Al_{10}Cu_{15.4}Ni_{12.6}$ had only ~0.5% inelastic deformation in compression. Samples reinforced with W, WC, and Ta exhibited substantial plasticity under compression (Fig. 3). The plastic strain of the tungsten reinforced samples was ~7%, whereas samples reinforced with Ta and WC showed less (~3–5%). The compression samples made from SiC particles and 3-μm W particles had no inelasticity.

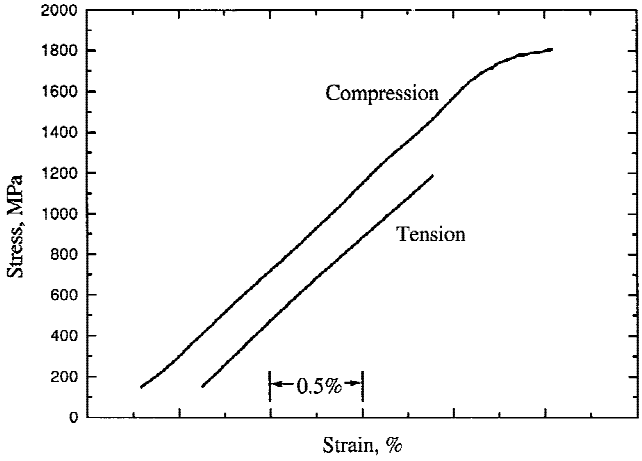

FIG. 1. Compression and tension stress–strain curves for $Zr_{57}Nb_5Al_{10}Cu_{15.4}Ni_{12.6}$.

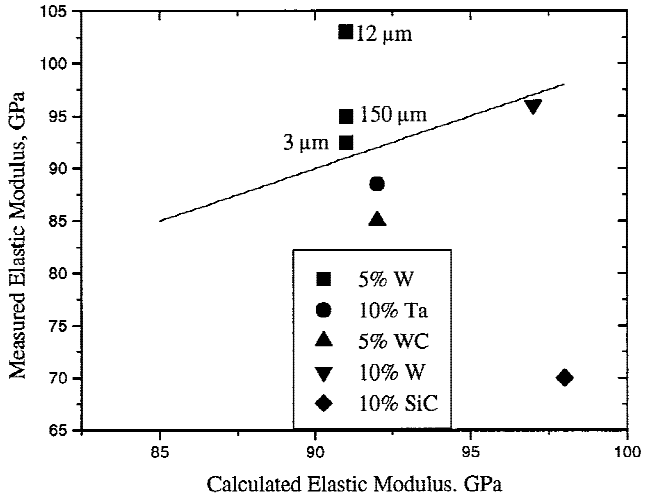

FIG. 2. Theoretical versus measured elastic modulus for $Zr_{57}Nb_5Al_{10}Cu_{15.4}Ni_{12.6}$ composites.

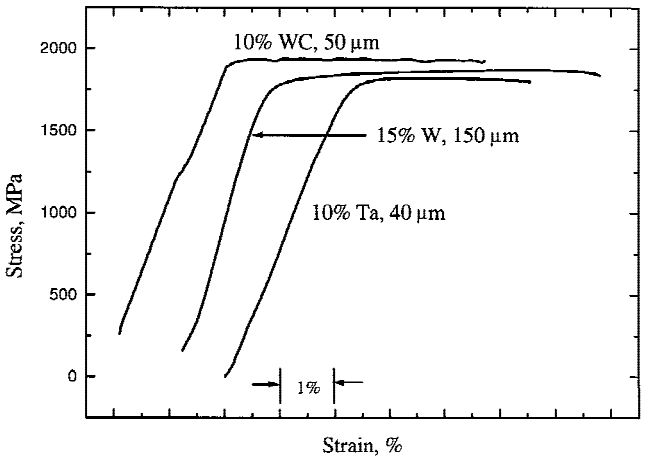

FIG. 3. Quasistatic compression stress–strain curves of $Zr_{57}Nb_5Al_{10}Cu_{15.4}Ni_{12.6}$ composites reinforced with Ta, W, and WC. A 15% V_fW provided the greatest strain to failure.

The compressive strength of the composites was equal to that of the unreinforced metallic glass. The ultimate strength of $Zr_{57}Nb_5Al_{10}Cu_{15.4}Ni_{12.6}$ in compression tests was 1.82 GPa, whereas that of the strongest composite sample was 1.96 GPa, a change of less than 8%. Strength did not vary significantly with particle size or volume fraction.

Unreinforced $Zr_{57}Nb_5Al_{10}Cu_{15.4}Ni_{12.6}$ and composites containing W, WC, and SiC were tested in tension. The 1.2 GPa tensile strength of unreinforced $Zr_{57}Nb_5Al_{10}Cu_{15.4}Ni_{12.6}$ is two thirds of the compressive strength (Fig. 1). There was no inelastic deformation in tension. Tungsten-reinforced composites had greater strength than $Zr_{57}Nb_5Al_{10}Cu_{15.4}Ni_{12.6}$ (Fig. 4), whereas composites containing WC and SiC had less. Although the stress–strain graphs of the composite samples show more curvature than the monolithic $Zr_{57}Nb_5Al_{10}Cu_{15.4}Ni_{12.6}$, none of the samples exhibit noticeable plasticity.

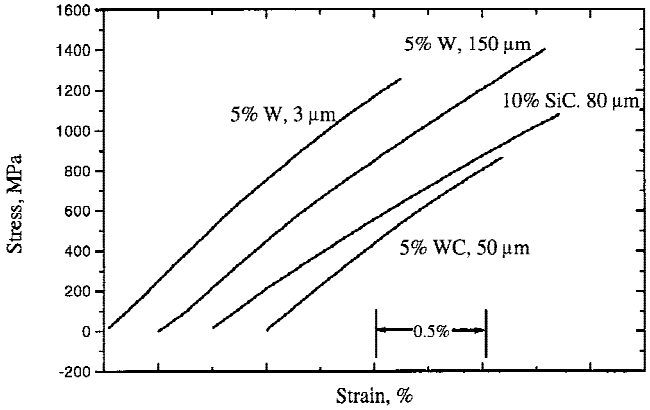

FIG. 4. Quasistatic tensile stress–strain curves for $Zr_{57}Nb_5Al_{10}Cu_{15.4}Ni_{12.6}$ matrix composites.

IV. DISCUSSION

The measured elastic moduli are typically within 7% of the theoretical values, calculated assuming spherical particles. Calculated modulus values would be approximately 15% higher for longitudinally aligned elliptical particles. However, according to Hasselman and Fulrath, dispersion shape has little or no effect on Young's modulus in a two-phase system when the modulus of the inclusion is greater than that of the matrix.[14] The elastic modulus of samples reinforced with 5% V_f tungsten particles varies with particle size. This is most likely the result of variation in reinforcement volume fraction (V_f), and scatter in the measurements. A 1% increase in reinforcement V_f results in a 1.5% increase in modulus. Particle size is not a variable in elastic modulus calculations. If elastic modulus depends on particle size, the modulus should vary in ascending or descending order with particle size. This is not the case with the experimental results.

The addition of particulate reinforcement greatly increased the plastic strain to failure, and hence the toughness, of the $Zr_{57}Nb_5Al_{10}Cu_{15.4}Ni_{12.6}$ metallic glass under compressive loading. This increase was the result of residual tensile stress in the matrix and the formation of multiple shear bands.

Residual stress develops within the composite on cooling because of the thermal strain that comes from the unequal thermal expansion of the particle and the matrix. The difference in thermal expansion, $\Delta\alpha = \alpha_p - \alpha_m$, is negative in all the composites tested. Thermal expansion coefficients are listed in Table I. The thermal strain, $\varepsilon_T = \Delta\alpha\Delta T$, was computed assuming the temperature change, $\Delta T = -400$ °C. This is the difference between room temperature, $T = 293$ K and the measured glass transition temperature,[15] $T_g = 693$ K. The thermal strain was used to calculate the average residual stresses. Because $\varepsilon_T > 0$, the particle is in compression, and the matrix is in tension. The residual matrix tensile stress

guides cracks toward the particles. The toughening of brittle materials with the addition of ductile particles is generally attributed to the particle applying a closure traction to the advancing crack front or to crack deflection.[16] In compression, however, no crack opening is present. In metallic glass systems under compression the particles resist shear loading, which retards shear band propagation.

The inelastic deformation in metallic glass is isolated to a narrow shear band. No plastic deformation would be visible if deformation was limited to a single shear band. The macroscopic plasticity demonstrated by the composite compression samples requires the generation of multiple shear bands. The isolated shear bands that initially form spread until encountering a particle. The shear stress, which is relieved during shear band propagation, builds around the particle, initiating additional shear bands in the sample. When the particle fails, the original shear band will continue to propagate. Multiple shear band formation in a compression sample can be seen in Fig. 5, an SEM photograph of the side of a WC-reinforced compression sample.

The behavior of the shear band slowing when encountering a particle, followed by fast fracture when overcoming the obstacle, is visible in Fig. 6, an SEM photograph of a W particle in a metallic glass matrix. It has been proposed that the "venous" pattern in the fracture surface of a metallic glass is the result of abiabatic heating in the shear band causing softening of the metallic glass.[17] In the photograph, one can see that the flow is from upper left to lower right; the particle is partially covered by the metallic glass, which appears to have flowed as a very viscous liquid across a portion of the particle when the shear band reinitiated. The area to the upper left, which is characterized by venous dimples, is

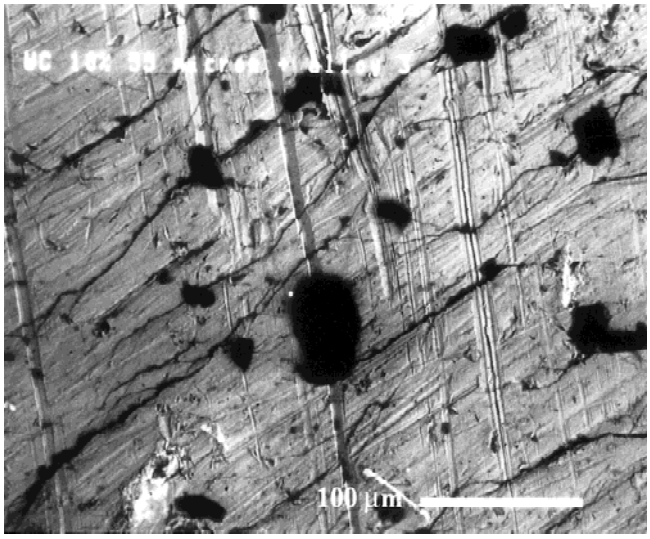

FIG. 5. Multiple shear band formation in a 10% V_fWC/$Zr_{57}Nb_5Al_{10}Cu_{15.4}Ni_{12.6}$ composite compression sample.

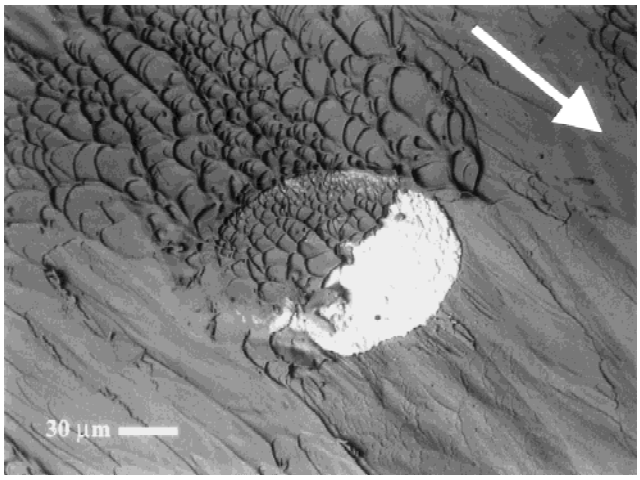

FIG. 6. Fracture surface of a W/$Zr_{57}Nb_5Al_{10}Cu_{15.4}Ni_{12.6}$ composite compression sample. Arrow indicates direction of shear band propagation.

where shear band movement would be most impeded. The areas to the sides and in front of the particle are smooth; this is interpreted as a region of fast fracture, occurring when the shear band overcomes the hindrance of the particle. This is consistent with the interaction of cleavage cracks with inhomogeneities in NaCl crystals.[18]

Figure 6 also reveals that the W failed in a brittle manner: the surface shows no microvoids or other evidence of ductile fracture. In the composite the particle is in a state of residual compression and highly constrained by the matrix. Particles fracture rather than deform because of this constraint.

Substantial compressive strain to failure was noted in all the samples except those made with SiC and 3-μm W particles. Composite samples reinforced with 150-μm W particles demonstrated the greatest strain to failure of any of the samples tested, whereas those of equal V_f made with 3-μm particles had none. Similarly, samples reinforced with 37-μm and 80-μm SiC were elastic until failure, whereas samples made from comparably sized W, WC, and Ta had sizable plastic deformation. It seems unlikely that the disparity in mechanical behavior is a function of particle size; it may be the result of processing. The 3-μm W particles did not wet readily during fabrication, which may have resulted in uneven particle distribution, particle "clumping," and voids. A portion of the SiC is likely to have dissolved into elemental Si and C. Silicon has been shown to affect the properties of Zr-based metallic glasses,[19] and the carbon readily forms brittle carbides with Zr.

The anisotropic mechanical behavior of $Zr_{57}Nb_5Al_{10}Cu_{15.4}Ni_{12.6}$ is in contrast to the isotropy of other Zr-based metallic glasses.[3] Although the composite strain to failure is substantially increased, the compressive strength is equal to that of unreinforced $Zr_{57}Nb_5Al_{10}Cu_{15.4}Ni_{12.6}$.

The residual matrix tensile stress in a 10% V_f WC composite is 18.9 MPa or about 1% of the compressive strength of the unreinforced metallic glass. This tensile stress must be overcome before compression of the matrix can occur, but this change is too small to explain the minor increase in compressive strength of some of the composites. All the composites have residual matrix tensile stresses but not all exceeded the compressive strength of monolithic $Zr_{57}Nb_5Al_{10}Cu_{15.4}Ni_{12.6}$. Also, theory does not support the contention that residual stresses cause a difference in tensile or compressive strength in particulate composites. Whether this small difference is the result of the reinforcement or scatter in the experimental results would require more study to determine.

Samples reinforced with W had similar strength regardless of particle size; 10% V_f W made with 150-μm particles had a (compressive) strength of 1.92 GPa, the same as that of samples with the same volume fraction of W reinforcement made from 3-μm particles. This resembles metal particle-reinforced oxide glass; the strength of Al reinforced soda-lime-glass in bending is independent of inclusion size.[20] The compression tests illustrate that failure stress is determined by the matrix strength and not the reinforcement.

Tensile strength in the W composites is up to 15% higher than monolithic $Zr_{57}Nb_5Al_{10}Cu_{15.4}Ni_{12.6}$. None of the tensile samples show the extensive plastic deformation of the compression samples. However, the energy to break (the area under the stress-strain curve), which corresponds to an increase in toughness, increased by more than 50% in some of the samples tested.

The energy to break is the energy per unit volume required to cause material failure and may be determined by integrating the stress–strain curve:

$$\frac{J}{m^3} = \int \sigma(\varepsilon) d\varepsilon$$

Numeric intergration of the tensile stress-strain curves gives an energy to break for unreinforced $Zr_{57}Nb_5Al_{10}Cu_{15.4}Ni_{12.6}$ of 873 MJ/m^3. The energy to break for the composite reinforced with 5% W (150-μm particles) is 1329 MJ/m^3, an increase of 52%. The ceramic particle reinforcements did not provide any significant increase in toughness. Silicon carbide-reinforced metallic glass showed an increase in area under the stress–strain curve of 5%, whereas the WC composite was substantially less.

Tensile samples of $Zr_{57}Nb_5Al_{10}Cu_{15.4}Ni_{12.6}$ also failed by 45 degree shear bands. The fracture surface (Fig. 7) consists of smooth regions linked by venous patches. This seems to be the pattern in metallic glass fracture surfaces: areas of fast fracture, characterized by a relatively smooth surface, connected by areas of slower crack growth, indicated by a heavier venous pattern. This

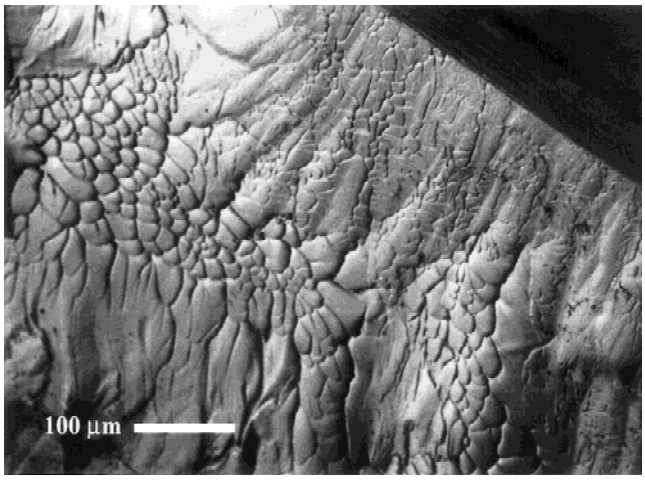

FIG. 7. Tensile fracture surface of $Zr_{57}Nb_5Al_{10}Cu_{15.4}Ni_{12.6}$ sample showing alternating regions of rough (slow) and smooth (fast) fracture.

fast/slow, smooth/rough pattern repeats across the fracture surface. This is similar to the surface features found in oxide glasses, in which fracture initiation is characterized by a very smooth, shiny mirror area and transitions to areas of increased roughness called mist and hackle.[21]

The fracture surface of a 5% W reinforced tensile specimen is illustrated in Fig. 8. It is jagged, with shear lips on both edges of the sample. The center section on the left-hand side of the sample is flat and smooth, but the right-hand side is coarse, with many protrusions.

The region of the shear lip is shown in Fig. 9. Shear lips are never present on unreinforced metallic glass. The flat surface of the particles reveals brittle fracture rather than ductile failure by microvoid coalescence. The change in matrix surface texture shows that the particles

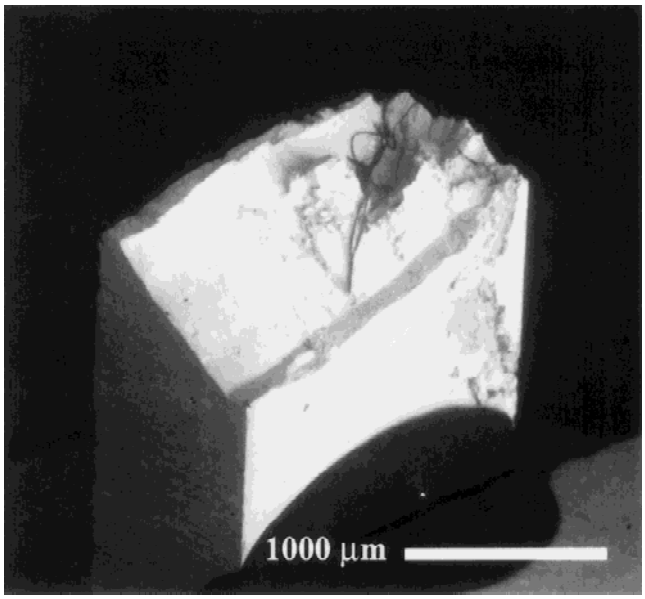

FIG. 8. Tensile fracture surface of 5% V_f W/$Zr_{57}Nb_5Al_{10}Cu_{15.4}Ni_{12.6}$ composite.

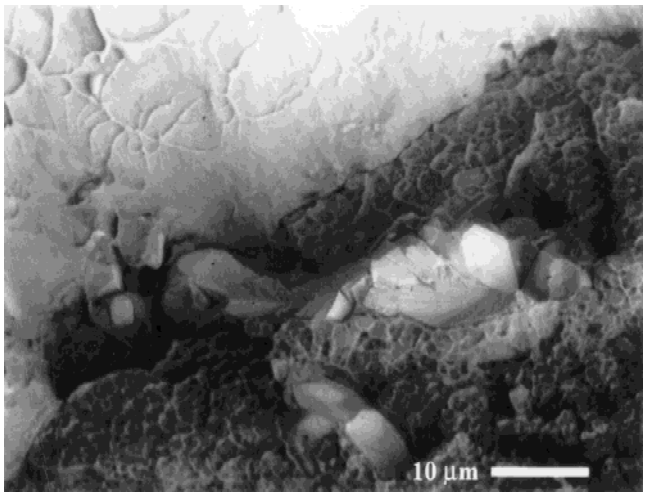

FIG. 9. Close-up of area around shear lip of 5% V_f W/$Zr_{57}Nb_5Al_{10}Cu_{15.4}Ni_{12.6}$ tensile sample in Fig. 8. Note the fractured W particle in the shear lip.

slowed initial crack propagation. Particles on the fracture surface either pulled out, leaving behind small craters, or were retained by the matrix and fractured. The numerous facets of the fracture surface are the result of multiple shear band propagation in the sample and greatly increase the total area of the fracture surface.

The toughening in the tensile case is attributed to two factors: the restriction the particles place on the propagating shear band, causing it to slow and change direction, and an increase in the surface area over which the fracture occurs. Two factors explain toughening in these systems:[22] first, the critical stress for shear band formation in the composite is larger than the monolithic glass because the particle/matrix interaction provides an additional restraint to shear band deformation; and second, if the shear stress remains constant and equal to that of the monolithic glass, the energy increment required to fracture a composite, because of the additional surface area, is on the order of 50% greater than that of the monolithic glass. This value is consistent with the results of the tensile experiment.

V. CONCLUSIONS

The addition of ductile particles increases the strain to failure of $Zr_{57}Nb_5Al_{10}Cu_{15.4}Ni_{12.6}$ metallic glass matrix compression samples through the formation of numerous shear bands. The tensile strength of unreinforced $Zr_{57}Nb_5Al_{10}Cu_{15.4}Ni_{12.6}$ metallic glass and composites using $Zr_{57}Nb_5Al_{10}Cu_{15.4}Ni_{12.6}$ as the matrix material is approximately two thirds of the compressive strength. Ductile particles provide a 50% increase in the toughness of the metallic glass in tension by obstructing shear band propagation and by generating additional fracture surface area. The metallic glass matrix flows as a viscous fluid within the shear band. The elastic modulus of the composites agrees with the values predicted by theory.

ACKNOWLEDGMENT

This work was performed with the support of the United States Army Research Office under Grant No. DAAH04-95-1-0233.

REFERENCES

1. K. Klement, R.H. Willens, and P. Duwez, Nature **187,** 869 (1960).
2. A. Peker and W.L. Johnson, Appl. Phys. Lett. **63,** 2342 (1993).
3. H.A. Bruck, T. Christman, A.J. Rosakis, and W.L. Johnson, Scripta Metallurg. Mater. **30,** 429 (1994).
4. A. Inoue, T. Shibata, and T. Zhang, Mater. Trans. JIM **36**(12), 1420 (1995).
5. D.J. Green, P.S. Nicholson, and D.J. Embury, J. Mater. Sci. **14,** 1413 (1979).
6. V.V. Krstic, P.S. Nicholson, and R.G. Hoagland, J. Am. Ceram. Soc. **64**(9), 499 (1981).
7. G. Baran, M. Degrange, C. Roques-Carmes, and D. Wehbe, J. Mater. Sci. **25,** 4211 (1990).
8. R.U. Vaidya and K.N. Subramanian, SAMPE J. **29**(4), 26 (1993).
9. H. Kato and A. Inoue, JIM **38**(9), 793 (1997).
10. H. Choi-Yim and W.L. Johnson, Appl. Phys. Lett. **71**(26), 3808 (1997).
11. J.D. Eshelby, Proc. R. Soc. London **A241,** 376 (1957).
12. J.D. Eshelby, *Progress in Solid Mechanics*, edited by I.N. Sneddon and R. Hill, 89 (North-Holland Publishing Co., Amsterdam 1961).
13. X. Lin and H. Choi-Yim (unpublished).
14. D.P.H. Hasselman and R.M. Fulrath, J. Am. Ceram. Soc. **48**(10), 548 (1965).
15. X. Lin, Ph.D. Thesis, California Institute of Technology (1997).
16. L.S. Sigl, P.A. Mataga, B.J. Dalgleish, R.M. McMeeking, and A.G. Evans, Acta Metall. **36**(4), 945 (1988).
17. C.A. Pampillo and A.C. Reimschuessel, J. Mater. Sci. **9,** 718 (1974).
18. C.T. Forwood and A.J. Forty, Philos. Mag. **11**(113), 1067 (1995).
19. H.A. Bruck, Ph.D. Thesis, California Institute of Technology (1995).
20. T.B. Troczynski, P.S. Nicholson, and C.E. Rucker, J. Am. Ceram. Soc. **71**(5), C-276 (1988).
21. *Fractography of Ceramic and Metal Failures*, edited by J.J. Mecholsky, Jr. and S.R. Powell, Jr., ASTM STP 827, 7, American Society for Testing and Materials Philadelphia (1982).
22. Y. Leng and T.H. Courtney, Metall. Trans. A **21A,** 2159 (1990).